

# The Lower San Fernando Dam

## 1 Background

There was a significant earthquake in Southern California in 1971, which is referred to as the San Fernando earthquake. The earthquake occurred on February 9, 1971 at 6:00 a.m. local time and had a 6.6 Richter magnitude.

The earthquake created a liquefaction failure at a water storage facility known as the Lower San Fernando Dam and Reservoir in the San Fernando community on the northern edge of the greater metropolitan Los Angeles area. Another facility known as the Upper San Fernando Dam also suffered some damage, but it was not as serious as at the Lower Dam.

Figure 1 shows an aerial view of the area. The Lower Dam is on the left side of the picture and the Upper Dam is toward the upper right of the picture. US Interstate Freeway 5 is on the right of the picture.



**Figure 1 The San Fernando dams a reservoirs**

The earthquake shaking initiated a major failure on the upstream side of the dam. The photos in Figure 2, Figure 3 and Figure 4 show some of the conditions after the earthquake. Of significance is the very steep slide head scarp (Figure 2) and very marginal freeboard the remained after the failure.

These photos are from Professor Ross W. Boulanger's web site photo album at the University of California, Davis, California. The web site link is:

<http://cee.engr.ucdavis.edu/faculty/boulanger/>

Presumably, based on the names on the photographs, they were taken by H.B. (Harry) Seed and J.M. (Mike) Duncan.

The failure led perilously close to a catastrophe. Had the head scarp been slightly lower, the outflow from the reservoir would have quickly eroded the dam and flooded many communities downstream. Considering the extremely precarious situation, some 80,000 people over an 11-square-mile area were evacuated while the reservoir was emptied over a period of three to four days.



**Figure 2 Upstream face of the dam after drawing down the reservoir**



**Figure 3 General view of the slide head scarp**



**Figure 4 A close-up view of the slide head scarp**

## 2 Case history

The San Fernando dams have become extremely important case histories for geotechnical earthquake engineering. Due to their significance, the cases have become the subject of years of research and numerous publications.

Much of the early research was done by Professor H. Bolton (Harry) Seed and his colleagues at the University of California at Berkeley. Their work led to three papers that provide much of the background information and early investigation findings. The three papers are:

- Seed, H.B., Lee, K.L., Idriss, I.M. and Makadisi, F.I. (1975). *The Slides in the San Fernando Dams during the Earthquake of February 9, 1971* – ASCE, J of the Geotechnical Engineering Division, GT7, pp. 651-688
- Lee, K.L., Seed, H.B., Idriss, I.M., and Makadisi, F.I. (1975). *Properties of Soil in the San Fernando Hydraulic Fill Dams* – ASCE, J of the Geotechnical Engineering Division, GT8, pp. 801-821
- Seed, H.B., Idriss, I.M., Lee, K.L. and Makadisi, F.I. (1975). *Dynamic Analysis of the Slide in the Lower San Fernando Dam during the Earthquake of February 9, 1971* – ASCE, J of the Geotechnical Engineering Division, GT9, pp. 889-911

Reference to these papers will be made as Seed et al. throughout this document. These papers were published in three consecutive months: July, August and September.

## 3 Purpose

In light of the importance of the San Fernando Dam case history and its prominence in the literature, it is important to show how GeoStudio, and in particular QUAKE/W, can be used to analyze a case like this. This example is intended for that purpose.

The purpose here is not to replicate all that has been done by others or to necessarily adopt the exact conditions presented by others, but to more generally illustrate the features and capabilities of GeoStudio in the context of a famous case history.

The emphasis here is on QUAKE/W because the cases involve earthquake shaking, but SEEP/W, SLOPE/W and SIGMA/W are also used for various aspects of the analysis.

## 4 Configuration and setup

The analysis the Lower Dam cross-section was idealized as shown in Figure 5. The dam height is 44 m with 2.5h:1v side slopes. The downstream side has a berm with a side slope of 4h:1v.

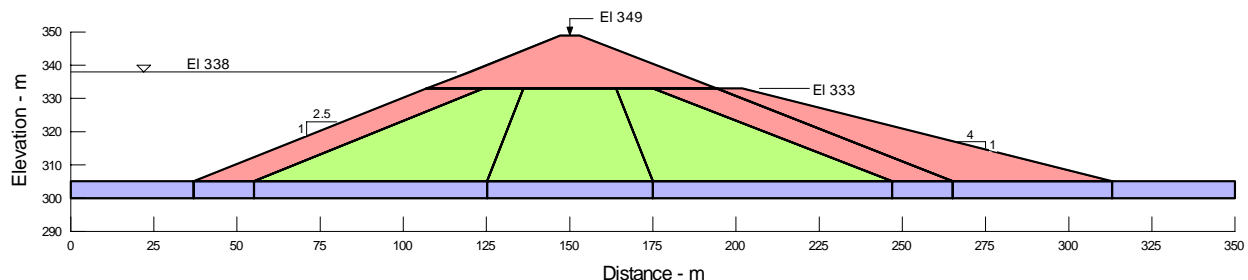


**Figure 5 Numerical analysis model of the Lower San Fernando dam**

The dam was constructed primarily by hydraulic fill placement. The fill was loosened in the borrow area by hydraulic jets of water and then transported to the site by means of wooden sluice troughs (Seed et al.). Dykes of dry fill were placed at the outer edges of the dam to contain the slurry. The material in these outer dykes was likely more dense and competent than the slurry fill in general, and this is the reason for the outer shell in the cross-section in Figure 5. The hydraulic fill placement was used to construct approximately the lower two-thirds of dam. The construction was completed by placing rolled fill on top of the lower hydraulic fill. The upper rolled fill apparently had minimal compaction (Seed et al.). Some time later a berm was constructed on the downstream side. A granular layer was placed between the original dam and the berm.

The dam was constructed directly on the stream-bed alluvium, which is about 5 m thick.

As one would expect from a hydraulic fill placement procedure and as was noticed during investigations after the failure, the fill graded from coarse silty sand at the outer edges to a more clayey soil towards the center.

#### **4.1 Clay core**

Seed et al. present the cross-section as having a clay core. For the analysis here, the entire hydraulic fill is treated as one material. The reason for this, as will be discussed below, is that the results this way give a picture closer to what actually happened. Furthermore, Peter Byrne in his R.M. Hardy Keynote address at the 2006 Canadian Geotechnical Conference in Vancouver suggested that stratification may have a significant impact on the potential for liquefaction. He looked at the impact of thin layers of clay amongst layers of loose sand and found that the impeded drainage resulting from the clay layers had a significant impact on the liquefaction response of the material in general. It is not difficult to imagine that there was some stratification at the Lower San Fernando Dam in the core area. Based on these more recent concepts, it is possible that there was some generation of excess pore-pressures and associated strength loss in the core area, just like in the remainder of the hydraulic fill.

Also, based on piezometers in the core area in the Upper San Fernando Dam, considerable excess pore-pressures developed in the core area during the earthquake shaking, further suggesting that the core area did not behave appreciably different than the hydraulic fill in general.

#### **4.2 Soil properties**

Soil properties for this analysis here are in large part estimates, filtered somewhat by values reported by Seed et al. In the end it turns out that when stability is the main issue, these estimated values are adequate to understand the observed behavior and processes.

Generally, the streambed alluvium, outer shell, top rolled fill, and downstream berm are treated as somewhat more competent as the hydraulic fill.

All of the details can be viewed and examined in the associated GeoStudio data file.

### **5 Liquefaction and the collapse surface**

Chapter 1 in the QUAKE/W Engineering Book presents a section on the Behavior of Fine Sand. This Section introduces the concept of a Collapse Surface. Figure 6 is one of the diagrams presented in Chapter 1. Fundamentally, any stress point such as Point B could experience the development of excess pore pressures during an earthquake until the mean effective stress  $p'$  reaches the collapse surface. Once on the collapse surface, the strength may fall down to the steady-state strength. On the other hand, the initial stress Point B in Figure 7 may experience the development of excess pore-pressures, but the

strength will never suddenly fall, since the initial deviatoric stress  $q$  is below the steady-state strength. This is discussed in more detail in the QUAKE/W Engineering Book.

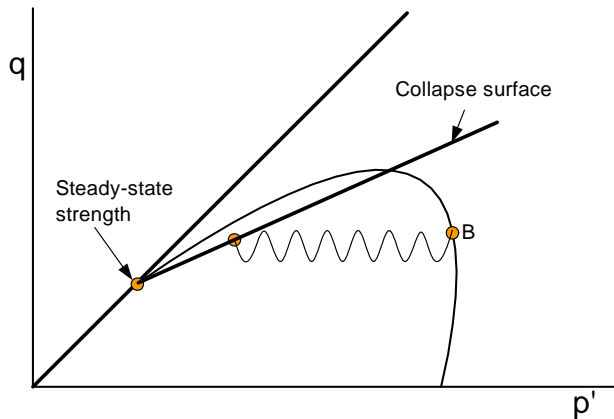


**Figure 6 Stress path of contractive loose sand**

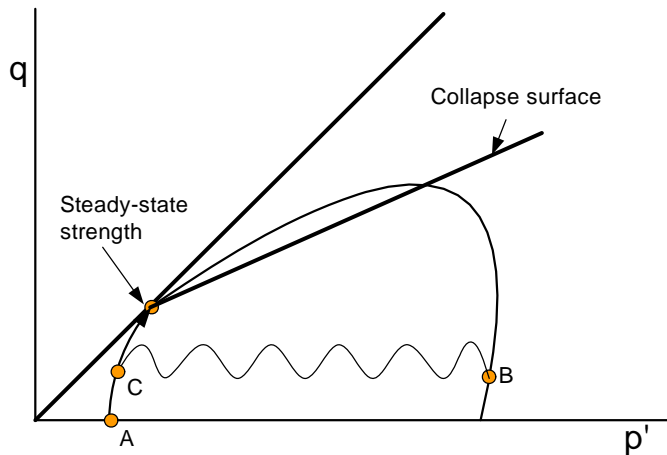


**Figure 7 Stress path of dense dilative sand**

QUAKE/W has an option to make use of the steady-state strength and the collapse surface to identify elements that can liquefy.

The user specifies the steady-state strength as  $C_{ss}$  and the inclination of the collapse surface.

$C_{ss}$  is multiplied by a factor of two to define  $q_{ss}$ , the steady-state deviatoric stress.

The slope of the Critical-State Line (CSL) is computed from,

$$M_{CSL} = \frac{6 \sin \phi'}{3 - \sin \phi'} \quad \text{where } \phi' \text{ is the specified effective friction angle.}$$

The slope of the collapse surface is computed the same way by substituting the specified collapse surface angle for  $\phi'$ . In the  $q$ - $p'$  space we can call the slope of the collapse surface  $M_{CS}$ . Once  $M_{CSL}$ ,  $M_{CS}$  and  $q_{ss}$  have been established, any  $q$  on or above the collapse surface can be computed for any  $p'$  value.

The rules adopted in QUAKE/W are as follows:

- Ratios of  $q/p'$  are computed for each element using the **initial** static stresses
- If  $q$  is less than  $q_{ss}$ , the element liquefaction flag is never set to “true”; excess pore-pressures can develop, but the element is not flagged as having liquefied regardless of the pore-pressures that develop
- If the  $q/p'$  ratio is such that the stress state is on or above the collapse surface, the element is flagged as having liquefied even before any earthquake shaking has started, since any small amount of shaking could cause the strength to fall down to the steady-state strength
- Elements with initial stress states such that  $q$  is greater than  $q_{ss}$ , but the stress points under the collapse surface are initially marked as not liquefied
- Stress points initially under the collapse surface will move to the left as pore-pressures develop during the shaking, and they are then marked as liquefied when the stress point is on or above the collapse surface

Excess pore pressures are limited or restricted, so that the mean effective stress  $p'$  is never lower than the  $p'$  corresponding with  $q_{ss}$  on the CSL. This prevents the effective stresses from becoming too low or even negative, which in turn reduces difficulties with numerical instability (convergence).

Castro et al. (1992) did an extensive study of the steady-state strength of the Lower San Fernando Dam hydraulic fill material. They concluded that the average undrained steady-state strength was between 30 and 40 kPa depending on the method used to obtain the strength. Based on this, a value of 35 kPa is used in the GeoStudio analyses presented here.

Little information is available in the literature on the slope of the collapse surface. It is definitely a value lower than the effective friction  $\phi'$ . Kramer (1996, p. 364) suggests that an approximation is about two-thirds of  $\phi'$ . For the analyses here a value of 20 degrees was arbitrarily chosen, which is about 0.6 of the  $\phi'$  (0.6 x 34).

## 6 Analysis: Initial PWP

The first step in the modeling process is to establish the long-term steady-state seepage conditions and pore-pressures. This can be done with SEEP/W. On the downstream side, the watertable is taken to be at the ground surface or at the surface of the alluvium. As noted earlier, a granular blanket was placed between the original dam and the downstream berm. Assuming that the blanket functioned as intended, the piezometric line will daylight somewhere in the granular blanket. This can be modeled by tagging the boundary between the dam and the berm as a potential seepage face.

Approximate conductivity functions and  $K_{sat}$  values are adequate for this steady-state analysis, since the piezometric surface is high up in the dam and much of the seepage flow is in the saturated zone. Also, the pore-pressure distribution is not sensitive to  $K_{sat}$ .

Figure 8 shows the resulting piezometric line (watertable) and total head contours (equipotential lines).

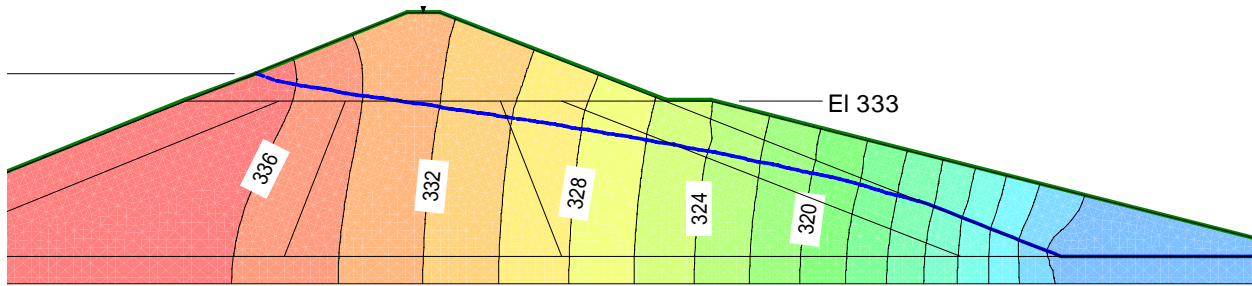


**Figure 8 Long term steady-state seepage and pore-pressure conditions**

## 7 Initial stress state

The next step is to establish the initial total and effective static stress distribution through out the dam. This can be done with a QUAKE/W Static-type analysis or a SIGMA/W Insitu analysis. The QUAKE/W Initial Static analysis type is used here.

To compute the initial static stresses, it is necessary to specify Poisson's ratio and the total unit weight of the soils. Remember that Poisson's ratio is used indirectly to say something about  $K_o$ , the remainder of the specified material properties do not influence the insitu stress calculations.

The previously computed SEEP/W pore-pressures are used in the static stress analysis.

It is important to include the weight of the reservoir water in the static stress analysis. This is done by applying a fluid pressure boundary on the region edges in contact with the reservoir. This is illustrated in Figure 9. The resulting vertical effective stresses are as shown in Figure 10.

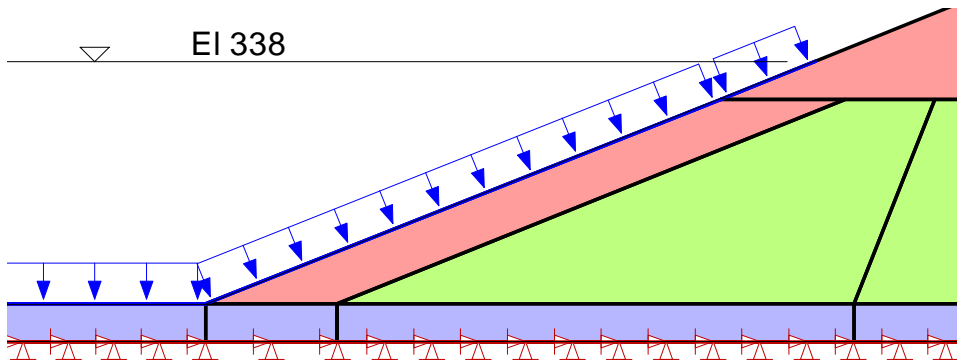


**Figure 9 The reservoir water weight boundary condition**

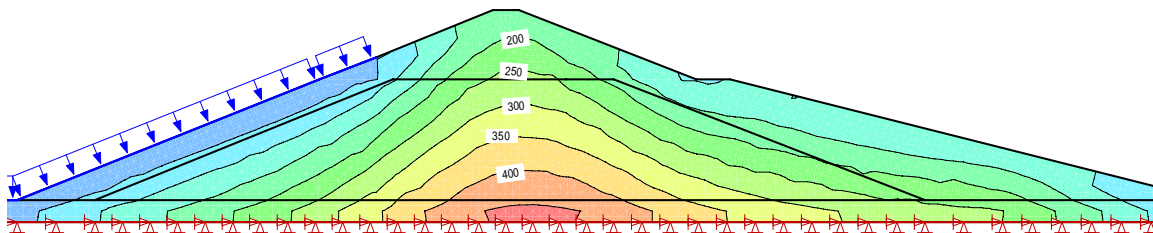


**Figure 10 Initial static vertical effective stresses**

## 8 Factor of safety under static conditions

As a reference point, it is useful to know the factor of safety under static conditions before the slide occurred. Based on the SEEP/W pore-pressures and QUAKE/W static stresses, the factor of safety is well above 2.0 as illustrated in Figure 11. Within the red band in this figure, the factor of safety is between 2.16 and 2.21. This is consistent with the findings by Seed et al., who concluded that the margin of safety against instability under the static conditions was fairly high.

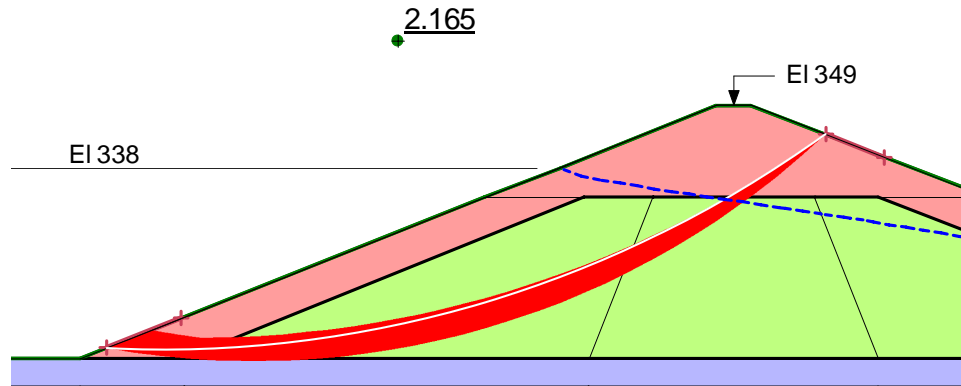


Figure 11 Stability before the earthquake

## 9 Analysis: Earthquake shaking

The next step is to do a dynamic analysis using QUAKE/W. The main purpose of the dynamic analysis is to determine the excess pore-pressures that may develop, and identify zones where the soil may have liquefied or where the soil strength may have dropped down to the steady-state strength.

The Equivalent-Linear method of analysis is used here.

### 9.1 Earthquake record

Time history records of the San Fernando earthquake are available from various seismic stations. Most of the past studies have been based on a recording station located on the abutment of the nearby Pacoima Dam located about 5 km east of San Fernando. The base rock peak acceleration at the San Fernando site has been estimated to be about 0.6 g and the record is scaled to a maximum 0.6 g to match this value. The time history record used in the analysis here is given in Figure 12. Small vibrations at the start and end of the publicly available record have been removed, limiting the total duration to 14 seconds, which includes all the significant peaks. The data points are presented at a constant 0.01 sec interval.

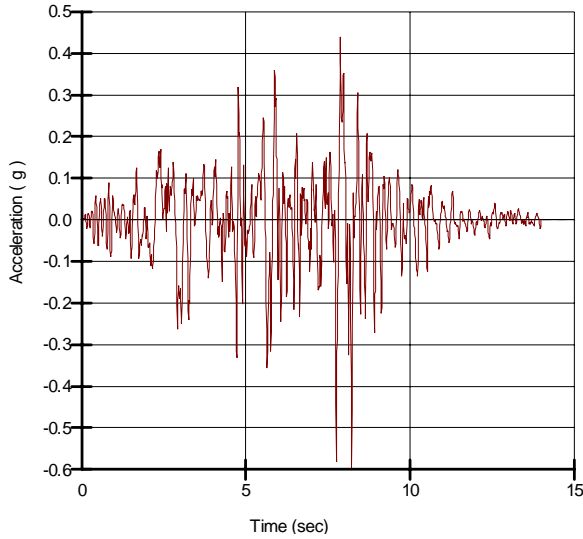


**Figure 12 Earthquake record based the station at the Pacoima Dam abutment**

## 9.2 $G_{max}$ moduli

The small strain shear moduli  $G_{max}$  are specified as functions. Figure 13 shows the function adopted for the hydraulic fill. The minimum value is 3000 kPa. Functions for the shell material and the alluvium have a similar shape but with a higher minimum value.

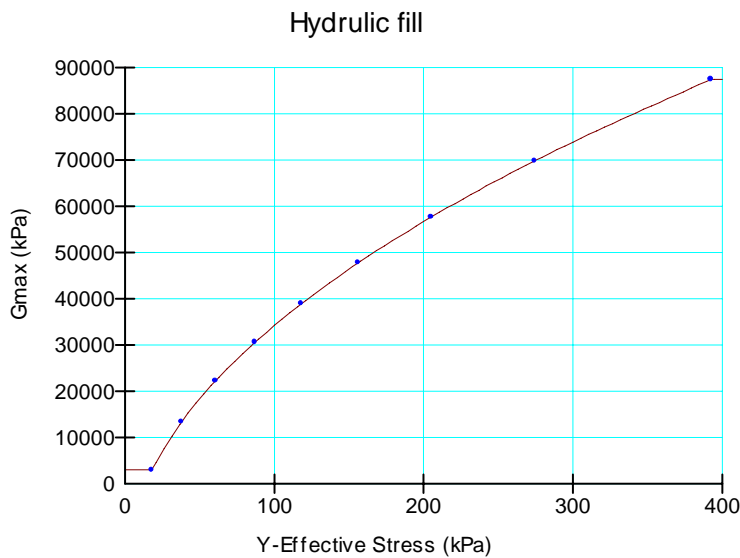


**Figure 13  $G_{max}$  function**

In an Equivalent Linear analysis the  $G$  modulus is modified based on the dynamic shear strains that develop during the shaking. The  $G/G_{max}$  function used for the hydraulic fill is shown in Figure 14.

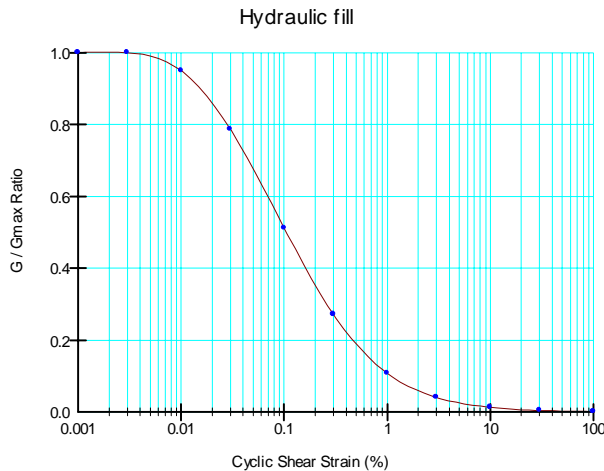


Figure 14  $G/G_{max}$  function for the hydraulic fill

### 9.3 Damping ratios

Typical damping ratios are defined and specified by functions such as the one shown in Figure 15.

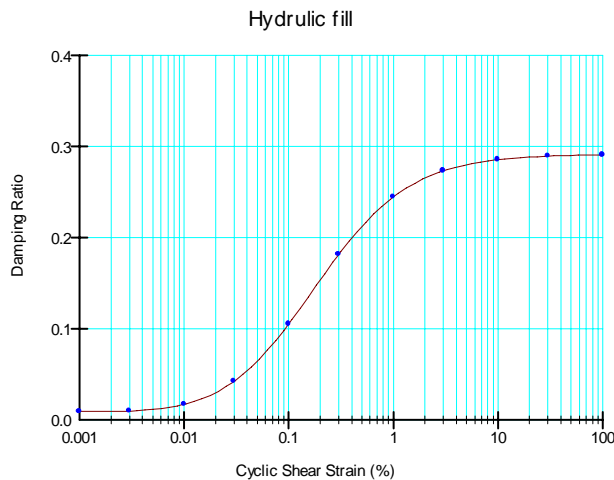
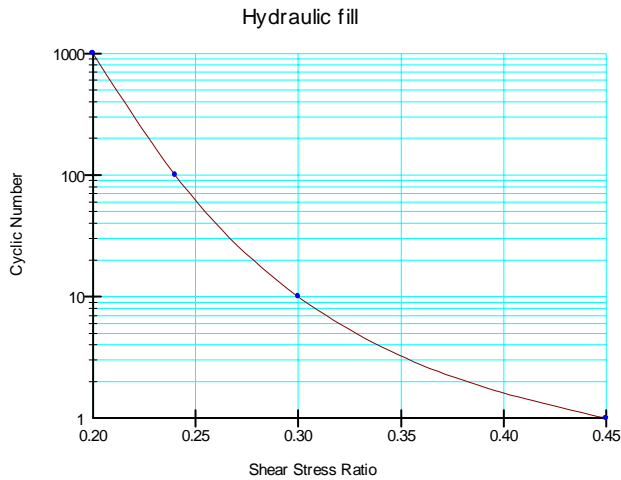


Figure 15 Typical damping ratio function

### 10 Pore pressure functions

The Equivalent Linear method of analysis in QUAKE/W is formulated to compute the generation of excess pore-pressures on the basis of Cyclic Stress Ratios (CSR), and on the basis of the number of uniform cycles experienced by the soil during the shaking, relative to the number of cycles required for the soil to liquefy. Two pieces of data have to be specified for this system. They are a Cyclic Number Function, such as in Figure 16, and a Pore-Pressure Ratio Function, such as in Figure 17.

Assume that the earthquake shaking produces the equivalent of 10 uniform cycles of shaking (details on this are given in the QUAKE/W Engineering Book). This is the number of cycles the dam will experience. Therefore, if the CSR in Figure 16 is 0.3 or greater, the soil will liquefy; that is, fewer than 10 cycles at a CSR or greater will produce liquefaction.



**Figure 16 Cyclic Number Function**

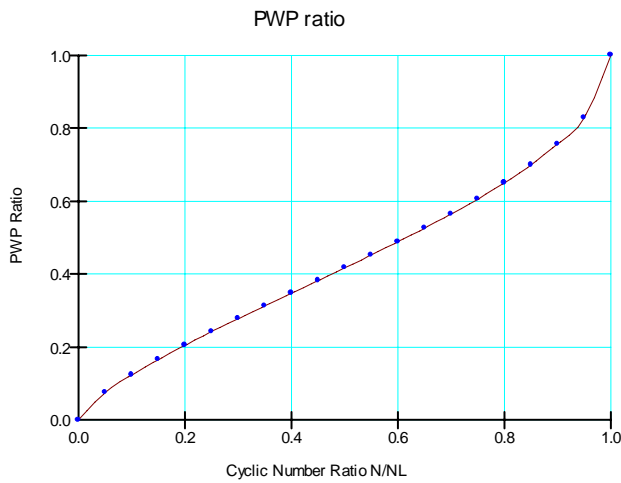


**Figure 17 Pore-pressure ratio function**

## 11 Dynamic response

History Points can be defined at selected points to get a complete picture of the dynamic response; that is, data is saved for each time-step integration point.

Figure 18 shows the response at the crest of the Dam. There is not much difference between this record and the input record in Figure 12. The peak at the crest is slightly less than the 0.6 g peak in the base record. In other words, there is no significant amplification or unrealistic damping. This is consistent with the conclusions reached by Seed et al.

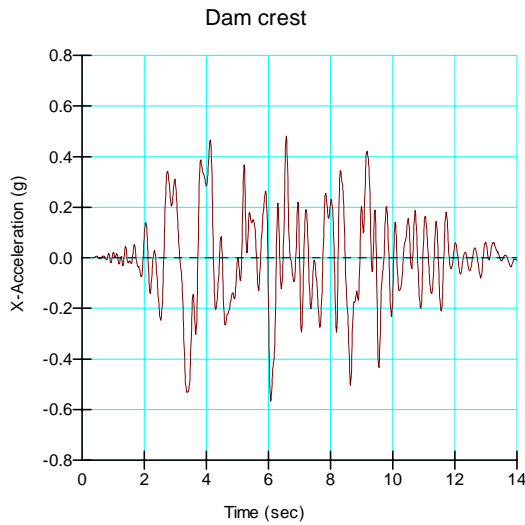


**Figure 18 Acceleration versus time at the Dam crest**

## 12 Liquefaction

Figure 19 shows contours of  $q/p'$  stress ratios under the initial static stresses. A point of significance is the high  $q/p'$  ratios in the central part of the hydraulic fill. This means that there is a zone where the initial  $q/p'$  points are above the collapse surface, as discussed earlier in Section 5. The soil strength in this zone could easily fall down to the steady-state strength with a small amount of shaking. With  $C_{ss} = 35$  and the inclination of the collapse surface at 20 degrees, stress ratios greater than about 0.9 indicate a stress point above the collapse surface. The yellow shaded area in Figure 20 is the zone where the stress ratios are initially above or on the collapse surface. In QUAKE/W this is flagged as a liquefied zone.

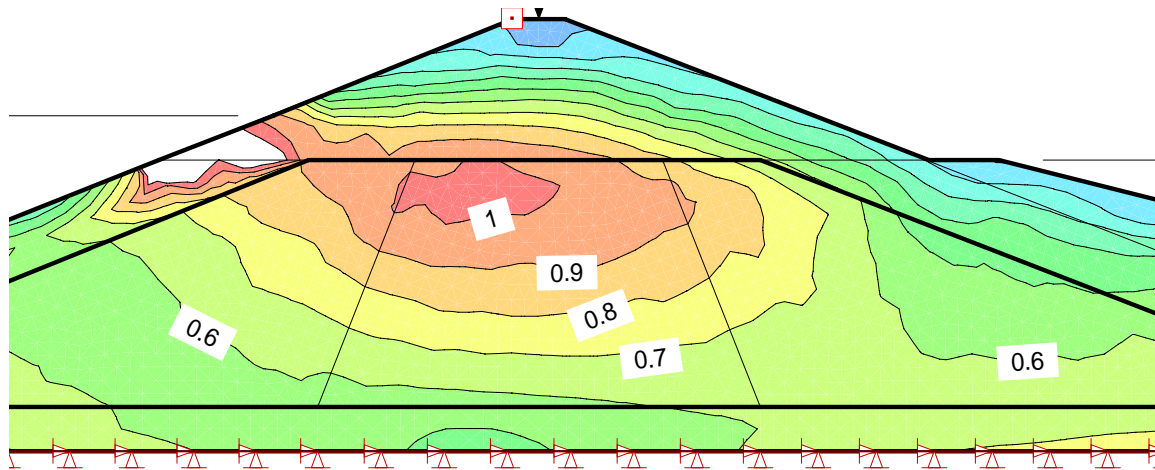


**Figure 19  $q/p'$  stress ratios under initial static stresses**

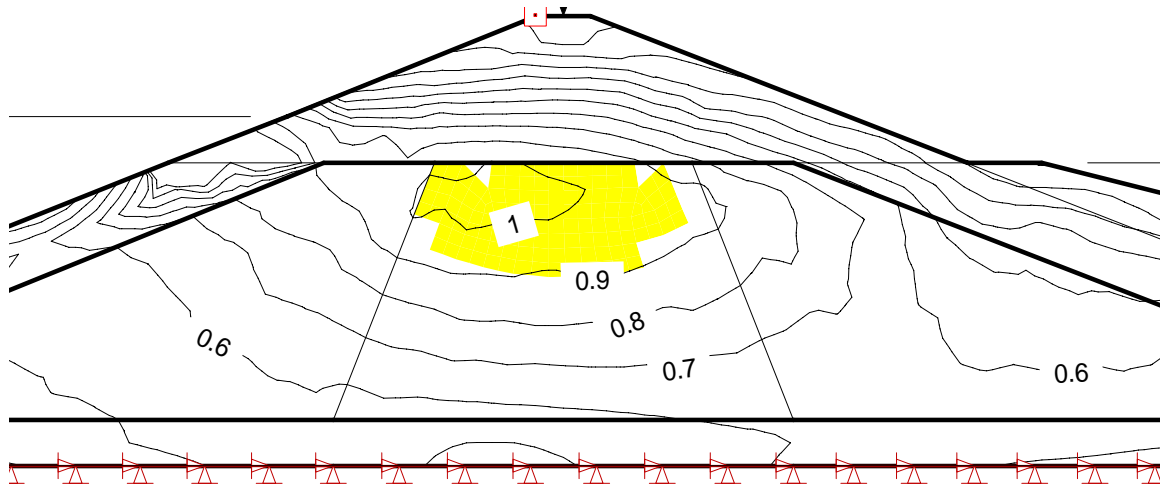


**Figure 20 Zone of liquefaction based on initial  $q/p'$  stress ratios relative to collapse surface**

During the shaking, excess pore-pressures will develop, causing other elements to reach the collapse surface as discussed earlier, or in other words, to liquefy. Figure 21 shows the liquefied zone at the end of the shaking.

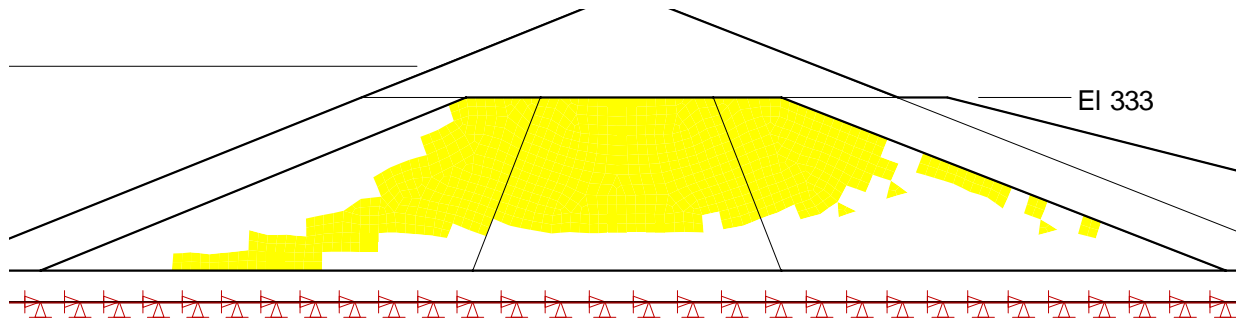


**Figure 21 Liquefied zone at the end of shaking.**

Of great significance is the shape and location of the liquefied zone on the downstream side. The shape and location is not unlike what Seed et al. determined what actually happened shown in Figure 22.

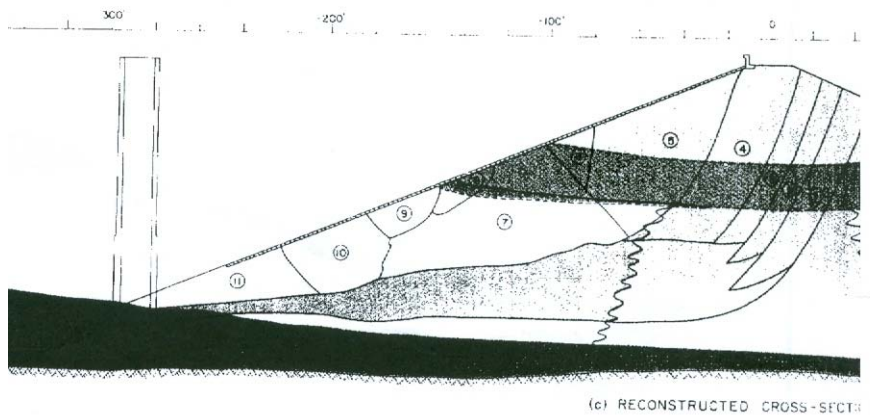


**Figure 22 Reconstructed section based on field investigations (after Seed et al.)**

They came to the conclusion that, in all likelihood, there was a tongue-shaped zone in the lower position of the hydraulic fill that was at the root cause of the liquefaction and subsequent instability. The QUAKE/W liquefied zone on the downstream side in Figure 21 is somewhat similar.

The liquefied zone in the core area is different than what Seed et al. believed to be the case. But in light of more recent research that has led to the concepts associated with a collapse surface and the impact that stratification may have had, as discussed earlier, it is not unthinkable that there was also a major strength loss in the core area. The QUAKE/W results suggest that this may have been the case.

### 12.1 Excess pore-pressures

Figure 23 shows contours of the excess pore-pressure at the end of the shaking. Of interest is the pocket of very high excess pore-pressures right in the tongue-shaped area Seed et al. considered to have liquefied. It is also of interest that this pocket is in a position where there could potentially be a slide slip surface.

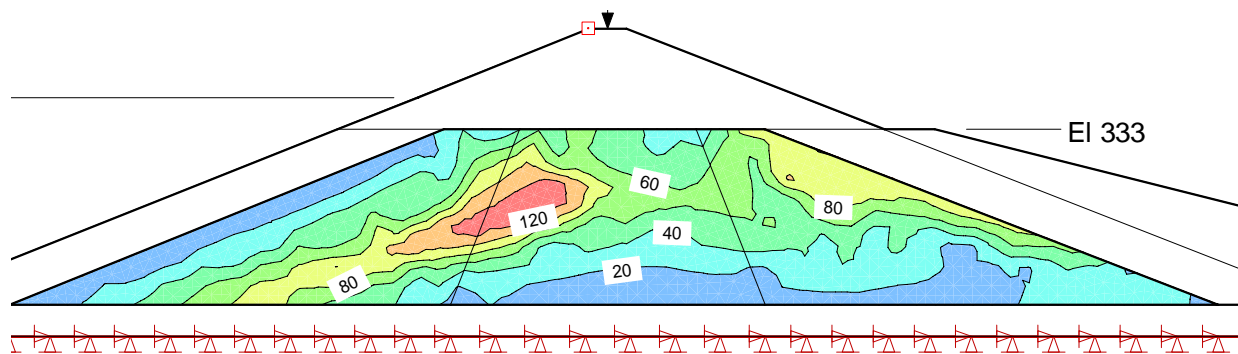


Figure 23 Contours of excess pore-pressure at the end of shaking

### 13 Post-earthquake stability

SLOPE/W has the capability to use the specified steady-state strength  $C_{ss}$  along the portion of a potential slip surface that passes through an element that QUAKE/W has marked as liquefied. Repeating the pre-earthquake stability analysis, but with post-earthquake pore-pressures and with  $C_{ss}$  strengths in the liquefied zones, results in a factor of safety of less than unity (1.0), which clearly was the case (Figure 24).

Figure 25 shows the cohesion and friction angle along the critical slip surface. Note how the cohesion jumps to 35 kPa and the friction angle drops to zero where the slip surface passes through liquefied elements (the toe is on the left and the crest is on the right).

As shown in Figure 26, the downstream margin of safety against failure remains fairly high in spite of the fact that the critical slip surface passes through some liquefied zones.

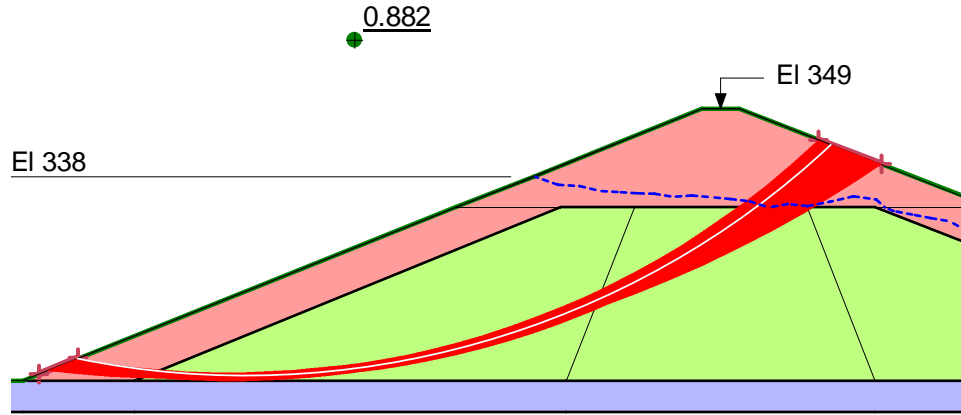


Figure 24 Post-earthquake stability

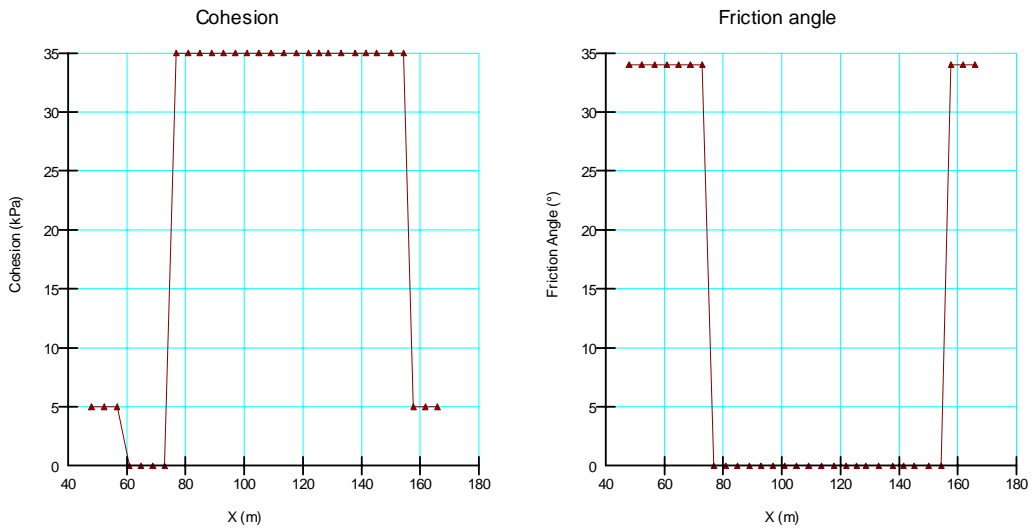


Figure 25 Cohesion and friction angle along critical slip surface

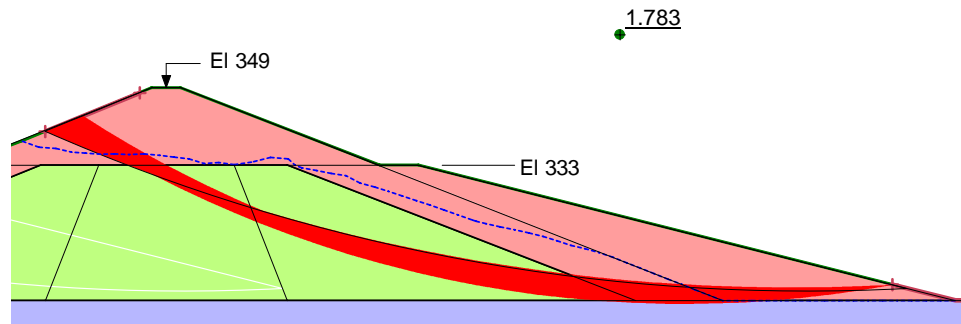


Figure 26 Downstream stability after the earthquake

## 14 Post-earthquake deformations

There is strong evidence that the major slide movements did not start until after the strong earthquake shaking. Seed et al. note that, "... the slide probably did not occur until near or just after the end of the stronger earthquake motions." The significance of this is that the inertial forces (mass times acceleration) had already vanished by the time the slide movement started. This being the case, the cause of the slide was the excess pore-pressures and the associated strength loss – not the inertial forces.

The post-earthquake conditions can be taken into SIGMA/W to do a stress re-distribution. Clearly some zones were over-stressed after the earthquake due to the strength loss. With SIGMA/W, it is possible to attempt to re-distribute the stresses in the over-stressed zones. Such a stress re-distribution generally is accompanied with deformations, especially when the overall structure approaches the point of limiting equilibrium. In this case it has already been shown that the structure was past the point of limiting equilibrium, but a stress re-distribution analysis can nonetheless provide some information about the failure mechanisms.

Figure 27 shows the displacement vectors from the post-earthquake SIGMA/W stress re-distribution. The movements seem to be a reasonable approximation of what happened as the movement started. In the crest area, the start of the movement is close to where the head scarp was, and the movements are downward at a steep angle, which is consistent with the actual head scarp as shown above in Figure 2. On the left side, much of the movement is more or less horizontal, which is also consistent with the observations presented in the published literature.

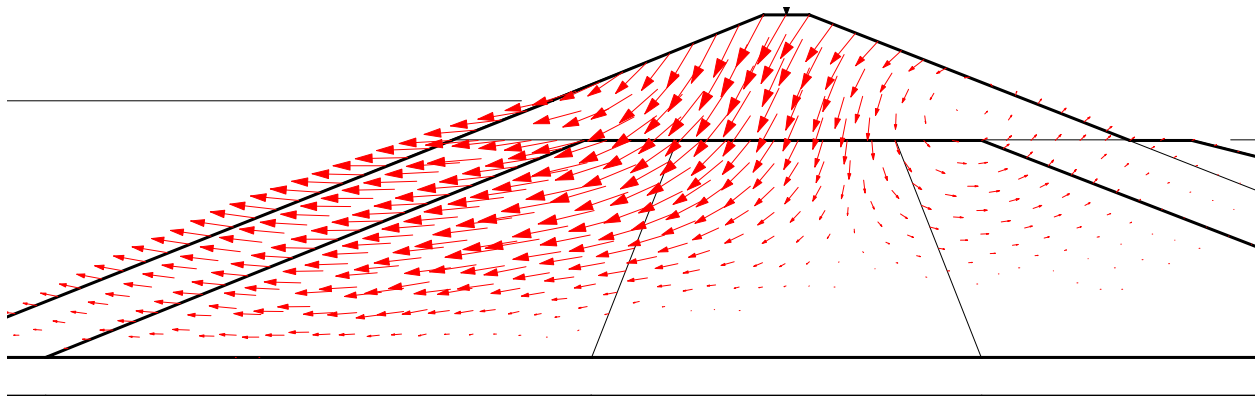


**Figure 27 Post-earthquake movement directions**

The actual SIGMA/W computed deformations are in excess of 70 m. This number is in and of itself meaningless in this particular case. The directions of the movement, however, are useful for understanding the failure.

Worth noting this is that the initial static stresses together with the final QUAKE/W pore-pressures are used for the stress re-distribution. The final QUAKE/W stresses may still include some remnant dynamic stresses, which should not be included in the stress re-distribution. Rather than prolonging the dynamic analysis to remove the remnant dynamic stresses, it is easier to just use the initial static stresses. The total stresses should be the same before and after the earthquake.

## 15 Closing remarks

This analysis of the Lower San Fernando Dam case history clearly demonstrates the advantages of the product integration in GeoStudio. Using QUAKE/W in conjunction with SEEP/W, SIGMA/W and SLOPE/W provides a much clearer picture than using QUAKE/W in isolation.

This analysis also shows that GeoStudio has all of the features required for analyzing the multiple issues inherent in a case like the Lower San Fernando Dam liquefaction failure.

Many of the material properties used in this analysis are simple estimates. They are, however, adequate for understanding the key issues and mechanisms. This is also true for any project. It is good modeling practice to first use realistic estimates of material properties to obtain an understanding of the key issues. Then a decision can be made as to where additional efforts and resources should be spent on further field investigations and testing.

## 16 References

Castro, G., Seed, R.B., Keller, T.O. Seed, H.B. (1992). *Steady-State Strength Analysis of the Lower San Fernando Dam Slide*, ASCE Journal of Geotechnical engineering, Vol. 118, No. 3, pp. 406-427

Seed, H.B., Lee, K.L., Idriss, I.M. and Makadisi, F.I. (1975). *The Slides in the San Fernando Dams during the Earthquake of February 9, 1971* – ASCE, J of the Geotechnical Engineering Division, GT7, pp. 651-688

Lee, K.L., Seed, H.B., Idriss, I.M., and Makadisi, F.I. (1975). *Properties of Soil in the San Fernando Hydraulic Fill Dams* – ASCE, J of the Geotechnical Engineering Division, GT8, pp. 801-821

Seed, H.B., Idriss, I.M., Lee, K.L. and Makadisi, F.I. (1975). *Dynamic Analysis of the Slide in the Lower San Fernando Dam during the Earthquake of February 9, 1971* – ASCE, J of the Geotechnical Engineering Division, GT9, pp. 889-911